Chem. Mater. **2002,** *14,* 915−917

Yttrium Oxide Nanoparticles Prepared by Alkalide Reduction

Jennifer A. Nelson and Michael J. Wagner*

Department of Chemistry, The George Washington University, Washington, D.C. 20052

Received September 19, 2001. Revised Manuscript Received November 9, 2001

Y_2O_3 nanoparticles have been synthesized by subambient homogeneous reduction using alkalide solutions and subsequent oxidation. As synthesized, the material consists of free flowing, well-defined 1−3 nm particles. Annealing in air at temperatures between 100 and 400 °C results in transformation of the material to irregular particles that are strongly agglomerated. Samples annealed between 500 and 800 °C consist of rather irregular, ill-defined, agglomerated particles while those heated to 900 °C consist of well-defined spheroids. Sintering occurs at temperatures as low as 100 °C, and crystallization is not observed until 500 °C. Samples annealed at 200 °C have surface areas of 109 m^2/g. Raising the annealing temperature from 500 to 900 °C results in a decrease of the surface area from 84 to 25 m^2/g while increasing the average crystallite size from 11.8 to 20.1 nm.

Introduction

Nanoscale Y_2O_3 powders are potentially important as precursors to films and nanostructured materials for a number of applications. Y_2O_3 stabilized zirconia films find application as thermal barrier coatings for gas turbine parts. They have been made by pressureless sintering of mixtures of the nanoscale components[1] and plasma spraying of powders.[2] Y_2O_3 films have been shown to be effective and mechanically durable antireflective coatings for large area CVD diamond optical components.[3] Y_2O_3 has been proposed as a replacement for SiO_2 for dielectric films in electronic devices. Y_2O_3 has a dielectric strength ($\kappa = 18$) that is more than 4 times larger than SiO_2 ($\kappa = 3.9$). The electrical leakage of amorphous Y_2O_3 films was found to be approximately 6 orders of magnitude better than SiO_2 and to display superior thermal stability.[4] Deposition on Si wafers by solution methods to produce films with good dielectric properties has been demonstrated.[5] Y_2O_3 doped with lanthanides shows promise for application as phosphors.[6−9] Finally, Y_2O_3 powders can be used as precursors for the preparation of dense ceramic objects.[10]

Alkalides are crystalline ionic salts consisting of crown ether or cryptand complexed alkali metal cations charge-balanced by a stoichiometric number of alkali metal anions.[11,12] Alkalides produce alkali metal anions when dissolved in nonreducible solvents. The alkali metal anion is nearly as thermodynamically powerful a reductant as a solvated electron, the most powerful reductant possible in any given solvent, and is capable of simultaneous two electron transfers. Alkalide reduction of metal salts results in the formation of a colloid of nanoscale (~2−15 nm diameter) particles. Colloid stability varies from minutes to hours, depending on the metal being reduced and the reaction conditions. After aggregation and removal of the solvent, the byproducts can be washed away, recovering the crown ether and leaving bare metal nanoparticles. Supported as well as bare particles can be produced.[13−16]

Alkalide reduction has been shown to be capable of producing alloys and compounds by co-reduction of two metals. In addition, the nanoscale metals have been used as precursors in nitride synthesis.[17] Here, we extend the method to the synthesis of Y_2O_3 by postsynthesis oxidation of Y metal nanoparticles during the removal of byproducts.

Experimental Section

Nanoscale yttrium metal was synthesized by homogeneous alkalide reduction according to the following scheme

---

* To whom correspondence should be addressed.

(1) Bhattacharya, S. S.; Betz, U.; Hahn, H. *Scr. Mater.* **2001**, *44*, 1553.

(2) Langjahr, P. A.; Oberacker, R.; Hoffmann, M. J. *J. Am. Ceram. Soc.* **2001**, *84*, 1301.

(3) Mollart, T. P.; Lewis, K. L. *Diamond Relat. Mater.* **2001**, *10*, 536−541.

(4) Kwo, J.; Hong, M.; Kortan, A. R.; Queeney, K. L.; Chabal, Y. J.; Opila, R. L. J.; Muller, D. A.; Chu, S. N. G.; Sapjeta, B. J.; Lay, T. S.; Mannaerts, J. P.; Boone, T.; Krautter, H. W.; Krajewski, J. J.; Sergnt, A. M.; Rosamilia, J. M. *J. Appl. Phys.* **2001**, *89*, 3920.

(5) Agarwal, M.; DeGuire, M. R.; Heuer, A. H. *Appl. Phys. Lett.* **1997**, *71*, 891.

(6) Silver, J.; Martinez-Rubio, M. I.; Ireland, T. G.; Fern, G. R.; Withnall, R. *J. Phys. Chem.* **2001**, *B105*, 948.

(7) Nishisu, Y.; Kobayashi, M. *Stud. Surf. Sci. Catal.* **2001**, *132*, 339.

(8) Bondar, V. *Mater. Sci. Eng.* **2000**, *B69−70*, 505.

(9) Holloway, P. H.; Jones, S. L. *J. Surf. Anal.* **1998**, *4*, 226.

(10) Hours, T.; Bergez, P.; Charpin, J. *Ceram. Bull.* **1992**, *71*, 200.

(11) Wagner, M. J.; Dye, J. L. *Annu. Rev. Mater. Sci.* **1993**, *23*, 223.

(12) Wagner, M. J.; Dye, J. L. Alkalides and Electrides. In *Comprehensive Supramolecular Chemistry*; Lehn, J. M., Gokel, G. W., Eds.; Elsevier: Oxford U.K., 1996; Vol. 1, p 477.

(13) Tsai, K.-L.; Dye, J. L. *J. Am. Chem. Soc.* **1991**, *113*, 1650.

(14) Dye, J. L.; Tsai, K. L. *Faraday Discuss.* **1991**, *92*, 45.

(15) Tsai, K. L.; Dye, J. L. *Chem. Mater.* **1993**, *5*, 540.

(16) Cowen, J. A.; Tsai, K. L.; Dye, J. L. *J. Appl. Phys.* **1994**, *76*, 6567.

(17) Chen, X. Z.; Dye, J. L.; Eick, H. A.; Elder, S. H.; Tsai, K.-L. *Chem. Mater.* **1997**, *9*, 1172.

10.1021/cm010900u CCC: $22.00

$$3K^+(15\text{-crown-}5)_2Na^- + 2YCl_3 \xrightarrow[-20\ °C]{THF} 2Y_{nano} + 3K^+(15\text{-crown-}5)_2Cl^- + 3NaCl \quad (1)$$

The byproducts were removed by washing with aerated H_2O at ambient temperature. This process oxidized the metal to Y_2O_3, without any apparent evolution of gas. The products were separated from the wash by centrifuge (15500× G).

YCl_3 (anhydrous, 99.99%, packed under Argon) was purchased from Aldrich and used without further purification. Crown ether (15-crown-5, 98%) was purchased from Alfa-AESAR, further dried, and then purified by vacuum distillation. Tetrahydrofuran (THF, 99.9+% HPLC grade, inhibitor free) was purified by stirring over KNa alloy until a persistent blue solution was obtained. Reaction vessel loading was performed in a N_2-filled drybox (<1 ppm H_2O and O_2), and solvent transfers were accomplished by vacuum techniques (10^{-6} Torr). Annealing was done in air in alumina combustion boats in a tube furnace. Further synthetic details can be found elsewhere.[13-17]

Electron micrographs were obtained on a JEM-1200EX transmission electron microscope (TEM) operation at 60 and 80 keV. Samples for TEM were dispersed in MeOH by sonication and deposited on Formvar holey film/carbon-coated copper grids. Powder X-ray patterns were obtained with a Scintag XDS-2000 diffractometer (Cu Kα radiation, 1.54 Å) equipped with a liquid N_2-cooled solid-state detector. Thermal analysis, differential calorimetric analysis (DSC), and thermogravimetric analysis (TGA) were performed on Perkin-Elmer Pyris DSC-1 and Pyris TGA-1 instruments, respectively, under flowing N_2 gas (20 mL/min). IR spectra were obtained with a Perkin-Elmer Spectrum RX FT-IR spectrometer.

Surface area measurements were made on a custom-built (in-house) adsorption apparatus using the BET method with N_2 as the absorption gas and the sample immersed in a liq N_2 bath. The system is based on classical designs and uses two burets with 11 Hg-filled bulbs to vary total volume. Pressure was measured with a MKS Instruments 870B capacitance manometer using a 660-B10 power supply/display. The vapor pressure of N_2 at the adsorption temperature (P_o) was measured directly with a Hg manometer. Samples that were annealed at temperatures of 500 °C and above were degassed for 4 h at 400 °C under vacuum (10^{-6} Torr) prior to adsorption measurements. Degassing of samples that were not previously heated was done for 8 h at 200 °C.

Results and Discussion

As synthesized at room temperature, the Y_2O_3 nanoparticles are in the form of a free-flowing, white powder. Powder XRD shows only broad features and selected area electron diffraction (SAD) patterns show only diffuse rings, indicating that the particles are amorphous or sub-nanocrystalline. Annealing for 4 h at temperatures as high as 400 °C resulted in no significant change in the XRD or SAD patterns. Annealing at 500 °C or higher, however, resulted in the appearance of peaks in the diffractograms that correspond to crystalline cubic Y_2O_3 (Figure 1). The XRD peaks sharpened with increasing annealing temperature, indicating crystallite growth (Figure 2). DSC studies of the heating process fail to reveal any thermal events associated with the crystallization, indicating a second-order thermodynamic process. Furthermore, as synthesized at room temperature, the product appears to be fully oxidized as no weight gain associated with oxidation is observed by TGA. FT-IR spectra of the products show them to be free of organic byproducts.

The crystallite size, as measured from X-ray line broadening, increases monotonically with temperature from an average of 11.8−20.1 nm for samples annealed at 500 and 900 °C, respectively. Surface area measured by the BET method, 109 m^2/g for materials heated to 200 °C, decreases monotonically with annealing temperature (Figure 3). Note that the particle size changes little (~3%) between 500 and 600 °C while the surface area decreases fairly dramatically (25%), which is indicative of sintering of the nanoparticles with little crystallite growth.

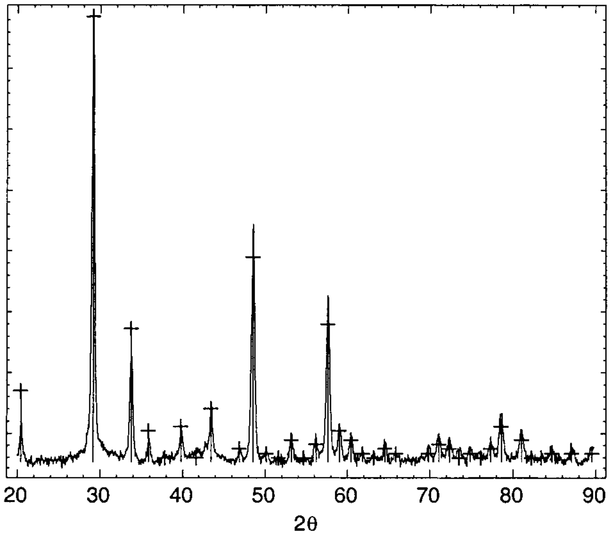

Figure 1. Powder diffraction pattern of Y_2O_3 nanocrystallites heated to 900 °C (solid line) and standard Y_2O_3 pattern (JCPDS PDF #41-1105, sticks with crosses).

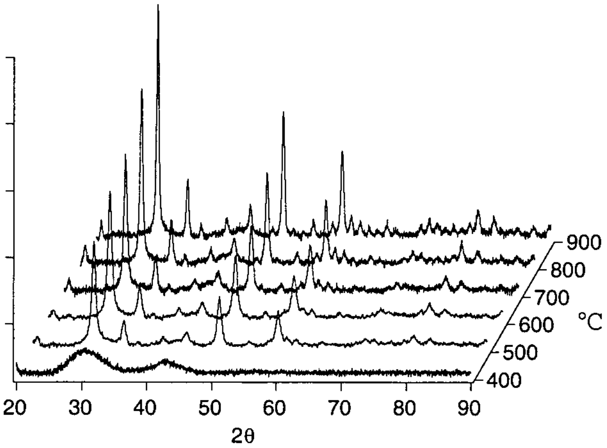

Figure 2. Powder diffraction patterns of Y_2O_3 nanocrystals heated for 4 h at the indicated temperature.

Unheated samples can be dispersed on TEM grids, showing individual, unagglomerated, and fairly regular nanoparticles with diameters of ~1−3 nm (Figure 4). Those annealed at temperatures from 100 to 400 °C form porous nanoparticulate films that densely coat the TEM grid. To obtain sufficiently transparent coatings for analysis, it was necessary to use highly dilute solutions. It is apparent that the particle size is significantly larger than that of unheated samples even after annealing at temperatures as low as 100 °C (Figure 5). However, due to the irregular shape and agglomeration of the annealed particles, it is difficult to make quantitative comparison other than to note that even the particles that appear to be the smaller particles within the agglomerates are more than twice as large as the average particle size of the unheated samples. Clearly, the particles have sintered without crystallization or,

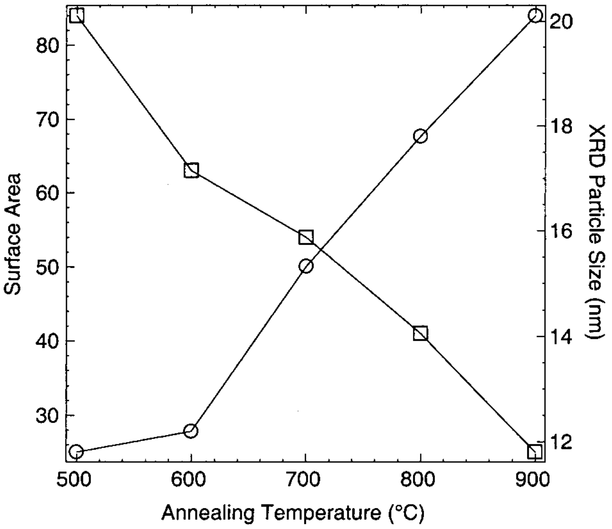

Figure 3. Surface area (squares), determined by BET adsorption measurements, and average crystallite size (circles), determined from XRD line broadening, as functions of annealing temperature. The lines connecting data points are to guide the eye. Samples were annealed for 4 h at the given temperature.

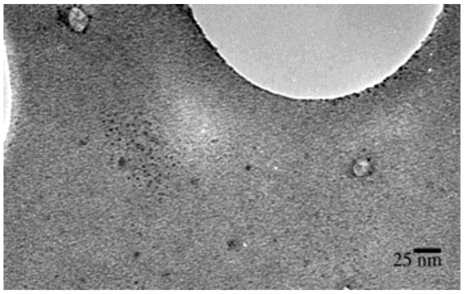

Figure 4. TEM micrograph of unheated Y_2O_3 nanoparticles.

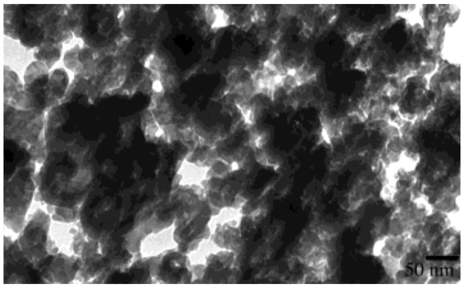

Figure 5. TEM micrograph of Y_2O_3 annealed at 100 °C.

if the sample is sub-nanocrystalline, without substantial crystallite growth.

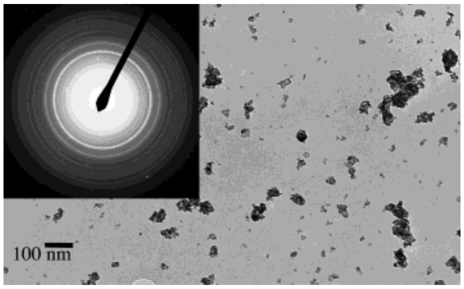

Figure 6. TEM micrograph of Y_2O_3 annealed at 500 °C. Inset is SAD pattern consistent with crystalline Y_2O_3.

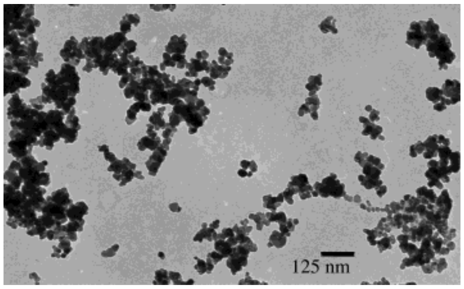

Figure 7. TEM micrograph of Y_2O_3 annealed at 900 °C.

The annealing of samples at 500 °C for 4 h results in crystalline material (Figure 6) that while still agglomerated, disperses with significantly less difficulty than samples that were subjected to lower temperatures. Morphologically, the samples heated at 500 °C are quite similar to those processed at lower temperatures, other than the markedly reduced tendency for complete TEM grid coverage. Raising the annealing temperature reduces the tendency to agglomerate and results in progressively more defined crystallites. However, even after heating to temperatures as high as 800 °C, the particles are still of highly irregular shape and far from perfectly defined.

The annealing of samples at 900 °C results in a transformation of the irregular crystallites into clearly defined spheroids (Figure 7). While still showing some tendency to agglomerate, individual crystallites can be easily distinguished within the groups. The observed crystallite sizes agree reasonably well with the average diameter measured by XRD line broadening.

Conclusions

Growth of dense Y_2O_3 films with materials made by alkalide reduction should be possible by drop-coating and sintering. Dense ceramics should be possible by consolidation. It is apparent that sintering occurs at temperatures as low as 100 °C. Amorphous films may be possible if annealing temperatures are kept below 400 °C. The heating at higher temperatures would result in crystallization but with the retention of relatively small crystallite size.

Acknowledgment. The authors thank Dr. Robin Rufner and the George Washington University Center for Microscopy and Image Analysis for assistance and use of the TEM imaging facilities. We also thank the National Science Foundation for financial support (DMR-9876164).

CM010900U